MDPI

Article

Thermal stratification and temperature variation in horizontal electric water heaters: A characterisation platform†

P.D. van Schalkwyk [1], J.A.A. Engelbrecht [1] and M.J. Booysen [1]

[1] Electrical and Electronic Engineering, Stellenbosch University, South Africa; mjbooysen@sun.ac.za

† This paper is an extended version of our paper published in 2021 IEEE International Conference on Electrical, Computer and Energy Technologies (ICECET), Cape Town, SA, 9-10 Dec 2021 [1]

Abstract: Electric water heaters, which have the capacity to act as thermal energy storage, are well suited to demand management strategies in smart grid applications. But finding the balance between managing power load, reducing thermal energy losses, user's convenience, and bacterial growth control, requires requires accurate modelling of the internal thermal dynamics of the tank. As a black box, this unknown is dependent on a multitude of environmental factors (e.g., ambient temperature and inlet temperature), water draw patterns, scheduling, set temperatures and orientation of the vessel. The latter affects the stratification and temperature variation inside the tank, and therefore has a direct bearing on the balancing act of demand management. Although these have been assessed inside vertically oriented tanks, what happens inside the horizontal variety – ubiquitous in developing countries – is currently left to the guesswork. In this paper we present the development of a platform with which the temperature variations inside a horizontal water heater can be characterised under numerous environmental and usage conditions. The importance of doing so is highlighted by the results, which clearly show substantial temperature variation along the vertical axis, and interesting phenomena along the longitudinal and transverse axes, for both static (no water draw) and dynamic (with water draw) conditions. We conclude by highlighting potential for further research.

Keywords: Thermal stratification; Electric water heaters; Thermostat control; Energy characterisation, Energy usage

Citation: Van Schalkwyk, P.D; Engelbrecht, J.A.A.; Booysen, M.J. Thermal stratification in horizontal electric water heaters: A characterisation platform†. *Energies* **2022**, *1*, 0. https://doi.org/

Received:
Accepted:
Published:

Nomenclature

Δt	Sampling period	V	Volume
c_p	Specific heat capacity of water	$\dot{V}$	Volumetric flow rate
E	Energy	Str	Stratification number
t	Time	Δz	Vertical distance between centre of layers
$\dot{Q}$	Heat transfer rate	M	First moment of energy
k	Thermal conductivity	j	Layer number
α	Thermal diffusivity	y	Distance from bottom of tank to centre of layer
ρ	Density	Pe	Peclet number
A_s	Surface area	H	Height of tank
T	Temperature	r	Radius of tank
$\dot{T}$	Rate of change of temperature	g	Gravitational acceleration constant
J	Number of layers (nodes)	β	Coefficient of thermal expansion

1. Introduction and background

Domestic electric water heaters (DEWHs) are considered to be one of the largest energy-consuming devices in a typical domestic household. In first-world regions such as Australia, the European Union and USA, water heating makes up 23%, 14% and 18% of the total residential load, respectively [2]. In South Africa, it can contribute to anything in a range of 30% to 35% of a household's total energy consumption, and accounts for approximately 7 % of South Africa's total grid load. [3–5].

It is no secret that electrical energy is a scarce commodity, especially in many developing countries that struggle to meet the ever-increasing energy demands. In Sub-Saharan Africa, approximately 600 million people still live without access to electricity, which is more than in any other part of the world [6].

Electric water heaters (EWHs) can be used for grid stabilisation purposes using demand side management (DSM) for peak shaving and energy saving [7]. There are at least 5.4 million of these heaters in the country [8], making them ideal candidates for demand response (DR) [9]. This provides the opportunity for struggling electricity generators, like South Africa's parastatal utility Eskom, to implement large-scale DSM techniques, such as ripple control, to control and limit the load on the electrical grid.

Xu et al. state on DSM and DR strategies, that "any reliable strategies aimed at controlling the demand from aggregated power usage of multiple water heaters should be based on accurate and representative energy models, which require a thorough and comprehensive understanding of the thermal behaviour for each individual water heater" [9]. An accurate model of the EWH is needed to simulate its thermal behaviour and power usage. These are often termed "thermal" models because they primarily simulate the electrical energy supplied to the heater and the amount of energy extracted from the heater (exergy). The objective of using such models is firstly to simulate grid demand based on individual (usually statistical) hot water draws, and secondly to allow centralised demand management to reduce the load on the grid without (a) sacrificing individual EWH energy savings, (b) increasing cold events experienced by the EWH user, and (c) prevent bacterial growth due to low temperatures in the tank [8,10]. From this, the load on the grid can be simulated and optimised when a network of these devices are connected. The scale of these simulations necessitates the implementation of thermal models that are computationally inexpensive.

One significant phenomena that contributes to variations in energy consumption in an EWH is thermal stratification. It can be described as the vertical separation of water regions due to density differences. Since the density of water is relatively sensitive to temperature changes, lower density regions would tend to rise above regions that have higher densities. This means that water regions with higher temperatures (lower density) would rise to the top, while lower temperatures (higher density) would tend to rest at the bottom of the tank. This phenomena is also known as the buoyancy effect and also occurs naturally in most large bodies of water, such as dams and rivers. The thermal stratification of the EWH device is an important factor to be considered when characterising the energy consumption of these devices [11–14].

There are many models and experimental data in literature that aim to characterise EWH devices. Most are designed for vertically oriented tanks, and not many for horizontal tanks. EWHs are mounted horizontally in many developing countries, which makes it important to also focus on models representing horizontal tank orientation.

2. Related work

Models from literature can be classified by the working principles that govern the model. Most are physics-based (white-box models), but more data-driven and grey-box models are being developed to improve general model accuracy and computational efficiency for large-scale control in smart grid applications. Furthermore, they can also be classified based on whether they support the characterisation of stratification. A few models and experimental contributions are discussed in this section.

2.1. Physics-based models

Diao et al. [7] present a one- and two-node transitioning, physics-based model for vertical EWHs. It incorporates two other models; the one-node (or single mass) model from Dolan et al. [15], and the two-node (or two-mass) model from Kondoh et al. [16]. The one-node model assumes that the entire body of water inside the tank is at a uniform temperature, whereas the two-node model divides the whole tank volume into two separate isothermal volumes - the upper, warm epilimnion and the lower, colder hypolimnion [17]. These are separated by a layer known as the thermocline. The transitioning model changes from the one-node model to the two-node model when a large water withdrawal event occurs and predicts the vertical position of the thermocline. This is to model for some degree of thermal stratification. Engelbrecht et al. [18] incorporated a similar one- and two-node transitioning model that was used in the development of optimal scheduled and heating control strategies.

Nel et al. [19] developed a computationally inexpensive model for a horizontal EWH that can be used for mobile and DR applications. The one- to two-node transitioning model from [7] was extended by Nel et al. to accommodate a horizontally-oriented tank. In addition, the standing losses are also calculated and the model is validated using 900 hours of experimental data, including energy measurements; all of which were neglected in [7], [15] and [16]. The results for energy usage estimation show an estimation error of 2 % and 5 % for schedule control and thermostat control respectively [19].

Xu et al. [9] developed a partial differential equation (PDE) model in effort to simulate the transient behaviour of a vertical EWH at different tank regions. The model was validated using 250 hours of experimental data captured with a setup equipped with six digital sensors; four evenly positioned inside the tank (from top to bottom) and two at the inlet and outlet. In addition, the usage water flow rate and ambient temperature were also measured. The simulated temperature values were in good agreement with the measured temperature values, however, the computational complexity of the model was significantly higher than the one- to two-node transition model presented by Diao et al. [7].

2.2. Stratification measurement and analyses

Leeuwner et al. [17] evaluated the accuracy of the model presented by Nel et al. in [19] which uses a two-node approximation for the thermal stratification of the water. It was compared with measured nodal temperatures and energy usage after recreating the same experimental sequence as in the original experiment by Nel et al. [19]. The results of the study indicate that the energy usage estimation of the model is seemingly accurate, but it underestimates the effect of thermal stratification in the tank - both in transient and steady-state conditions [17]. The upper node temperature was hotter, and the lower node temperature, cooler, than the simulated results. One concern that arises from this conclusion is, again, that the lower region of the EWH might be a conducive region for the growth of a pathogen termed *Legionella*.

Farooq, et al. [14] developed a grey-box model of a low pressure electric boiler (similar to a vertically-oriented EWH) to predict the temperature dynamics within the tank for static and dynamic scenarios. Measurements of the internal temperatures were captured at 8 different equally-spaced locations in a vertical tank. The volume of the tank was 300 L and a 3 kW element was used to heat up the water. In their results, they concluded that during static heating, all layers within the tank heat up with a constant rate (even the bottom layers of the tank) and that during water consumption, the layers cool down in an orderly fashion from the bottom to the top as the colder water moves up in the tank [14]. Their model accurately predicted the temperature dynamics of the tank during a static heating scenario and for a water consumption scenario.

Fernandez-Seara et al. [13,20] wrote a two-part article series on experimental analyses of static and dynamic modes in vertical domestic electric hot water storage

tanks with a featured focus on the degree of stratification in the tank. Eleven temperature sensors were installed along the height of the tank to a probe depth of 20 cm.

The aim of the static mode analyses, as seen in [13], was to determine the internal thermal behaviour of a 150 L vertical EWH during static heating and static cooling modes and how it affects the efficiency of the system. The control parameters for the analyses were heating power, inlet water temperature and operating pressure. The results show that there is a clear indication of thermal stratification present. The temperature differences between the measured layers at the lower region of the tank increase with an increase of thermal power injection and/or an increase of operating pressure during a static heating mode. For static cooling, the results show that the lower regions of the tank heat up slightly due to thermal diffusion with the hotter epilimnion region. In addition, they observed that the entire cooling process occurs faster at an operating pressure equal to the water line pressure as compared to atmospheric pressure.

The second part of Fernandez-Seara et al. [20] investigated the degree of stratification of the same tank used in [13] for a dynamic mode of operation. They introduced six different inlet-outlet port configurations and three different water flow rates as control parameters. Their results show the upward movement of the thermocline region as a function of dimensionless time and vertical position of the tank. It is clear from the results that inlet-outlet configurations have a significant influence on the profile development of the thermocline as a function of time during a dynamic mode. In addition, it can be seen that the rate at which the the thermocline region moves upward is relatively constant between dimensionless times of 0.2 and 0.8 for lower water flow rates.

Chandra et al. [11] and Castell et al. [12] provide comprehensive reviews of stratification analysis techniques and the utilisation of useful dimensionless numbers to help characterise the degree of stratification in EWH tanks. It is clear that the exergy efficiency of the tank is directly proportional to the degree of stratification in the tank. If the hot water inside the tank mixes with the colder regions, the available energy at the outlet of the tank is lower, thus decreasing the exergy efficiency and creating thermodynamic irreversibilities. This is corroborated by results obtained by Fernandez-Seara et al. [20]. The inlet-outlet port configuration that yielded the highest degree of stratification had the highest discharging exergy efficiency for all flow rates used. This confirms that the degree of stratification is directly proportional to exergy efficiency and should be a variable to optimise. This is also observed in the numerical CFD results obtained in Abdelhak et al. [21].

Castell et al. [12] used and compared multiple numerical parameters to evaluate the efficiency and the degree of stratification of a vertically-oriented thermal energy storage tank. They state that the flow rate and the working temperature are the dominant factors that affect the stratification within a tank. Although the MIX number is considered to be good metric for characterising stratification, it is too sensitive to small temperature changes in the working temperature. As an improvement, they found that the Richardson number in combination with the Peclet number was a good metric by which to classify the thermal stratification.

Chandra, et al. [11] provide a detailed review of thermal stratification within DEWH tanks. They state that the thermal performance of any thermal energy storage (TES) device is optimised when the degree of stratification is high. In other words, when there is a distinct thermal boundary, known as the thermocline, separating the hot water region from the cold water region in the tank. A well-stratified tank has the potential to deliver higher exergy at its load side and has improved degrees of utilisation [11]. This is supported by the work done by Rosen, et al. [22] and by the converse observation that when hot and cold regions are mixed, the available energy at the load side of the tank decreases owing to the high thermal energy at load side diffusing to the colder regions of the tank.

2.3. Computational fluid dynamic (CFD) models

Thermal modelling tools, such as 'TRNSYS' and 'ANSYS Fluent' are used in many areas of research and industry. For example, Yildiz et al. [2] used TRNSYS to simulate the thermal stratification in a vertical EWH tank using 6 different isothermal zones. Their study used a data set consisting of energy measurements from 410 different households located in Australia. This was used to investigate the potential of storing excess photovoltaic (PV) generation in EWH devices. The results show that 48 % of hot water draw in a typical Australian household can be provided by excess PV generation.

Abdelhak et al. [21] developed CFD models for a vertical and horizontal domestic hot water storage tank for dynamic modes of operation. The numerical results of the CFD model were validated using the measured results from Fernandez-Seara et al. [20]. However, for the horizontal tank, the vertical model was merely rotated and used to compare the two orientations. The results show that the discharge efficiency of the tank in a horizontal orientation is lower than that of the vertical orientation and that the degree of stratification is also lower in the horizontal orientation. This appears to show that vertical tanks are typically more efficient than horizontal tanks in dynamic modes of operation.

Stone et al. [10] developed a CFD model of a horizontal EWH to simulate the temperature stratification and velocity fields that influence the motion and growth of resident microbes [10]. The results from the model clearly show that the lower region of the tank remain at temperatures below 45 °C creating opportune growth regions for *Legionella* (expanded on in Section 2.4 below). The physical measurements obtained and shown in this paper corroborate this and indicate that the temperature in the lower layers of the tank do remain significantly lower than the rest of the upper regions, especially during a static heating phase. However, further validation of the CFD model is required since crude assumptions were made about the thermal stratification inside the water tank. From their study it is clear to see that thermal stratification is an important consideration for EWH characterisation models.

2.4. Health considerations

Even though a high degree of stratification is optimal for energy optimisation, Stone et al. [10] and Armstrong et al. [23] state that lower temperatures in the hypolimnion region of an EWH may lead to environments conducive to the growth of microbial pathogens, such as *Legionella pneumophila*, which may lead to health risks. "This pathogen is the most notorious, responsible for respiratory diseases such as the milder Pontiac's fever and the more severe Legionnaires' diseases" [10].

It has been reported that intelligent schedule control and lowering of the EWH thermostat's target temperature can reduce energy usage by 29 % [24]. However, it is possible that the resulting internal temperature distribution after the application of any energy saving scheme, may also create an environment conducive to the growth of *Legionella pneumophila* [10,23]. This limits to exergy optimisation since a high degree of stratification will consequently lead to low hypolimnion temperatures.

Having said that, it is clear that an optimal operating point needs to be investigated between high exergy efficiency and little to no microbial growth in the hypolimnion regions of a horizontal EWH tank. In addition, the comfort, peak-load and energy usage, as discussed in Roux et al. [8] also need to be considered. The troika of challenges visualised by Ritchie et al. [25] could therefore be extended to incorporate the optimisation of energy with the consideration of microbial growth mitigation.

An EWH heating control strategy that considers and mitigates the growth of this pathogen is introduced in Engelbrecht et al. [18]. This strategy, termed *scheduled control with energy matching and Legionella sterilisation (EML)*, utilises scheduled control with energy matching and mitigates the impact of *Legionella pneumophila* by sterilising the water in the tank. This is done by heating the water up to and keeping it at 60 °C for at least 11 min before the largest water draw event of the day.

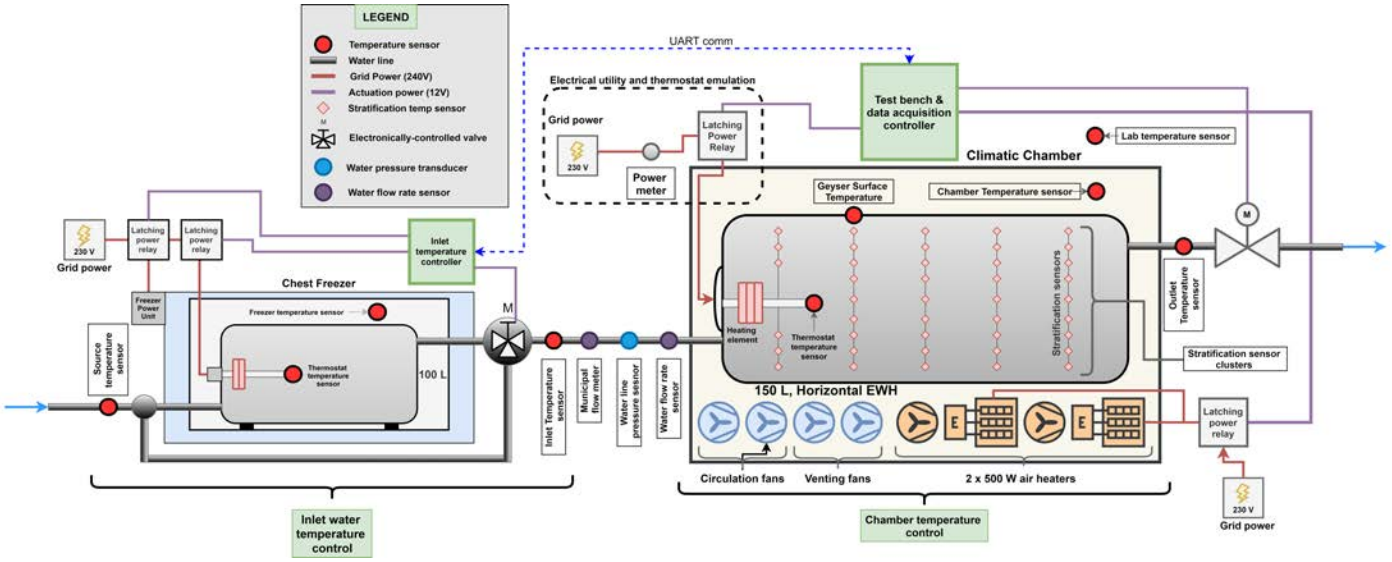

Figure 1. Experimental setup of EWH characterisation platform.

2.5. Contribution

This paper introduces the development of a platform for the characterisation of stratification in a commonly-used horizontal electric water heater, as shown in Figure 1. The platform incorporates multiple internal temperature sensors inside a horizontal water heater's tank. Additionally, the platform (1) emulates and controls the environmental conditions, such as ambient temperature and inlet water temperature, (2) emulates the electrical control (e.g. by the utility in DSM applications or the user in energy-savings efforts) and measures the resulting electric energy usage, (3) emulates the thermostat control with an electronically-controlled thermostat, and (4) emulates the user with schedule-, volume-, and flow-rate controlled water draw.

Physical temperature measurements of more than two nodes in horizontal EWH tanks are not documented in literature to the best of the authors' knowledge. This creates an opportunity to conduct experiments similar to those in [12–14,17,20,26] and to validate results from numerical models of horizontal EWH tanks such as ones developed in [10,19,21]. The experimental data acquired from the platform can be used to develop and train new machine learning models and/or develop state estimation (grey-box) models for horizontal EWH characterisation.

3. Experimental platform setup and design

The experimental platform, shown in Figure 1, is designed to control the variables that have an influence on the stratification in the tank, and consequently the energy characteristics of the EWH. Nel et al. [27] observed that a 5 % increase in the inlet water temperature can produce energy savings up to 13 %, and 5 % energy savings for the same change in ambient temperature. The results from Fernandez-Seara et al. [20] and Castell et al. [12] show that lower water flow rates improve the degree of stratification and thus improving exergy efficiency. Booysen et al. [24] found that 29 % energy savings can be achieved by using intelligent scheduled control and by lowering the thermostat set temperature. This is corroborated by Kizilors et al. [26] who observed that discharge efficiencies increase when thermostat set points are lowered. Clearly, these environmental conditions, water usage characteristics and switching patterns of the heating element have a significant influence on EWH thermal behaviour and energy characteristics.

Therefore, to characterise EWH thermal behaviour, the platform is designed to emulate and control the ambient temperature using a climatic chamber, emulate the

inlet water temperature using a controllable, in-line water heat exchanger, emulate the behaviour of the user by controlling water usage patterns and control the electrical switching frequencies and conditions for the heating element. Another significant objective of the experimental platform is data acquisition of the thermal stratification inside the tank, outlet water temperature for exergy analysis, environmental temperatures; ambient and inlet water, energy usage and water usage.

3.1. Environmental emulation

The ambient temperature and inlet water temperature are two dynamic factors that make up the environmental conditions that influence the thermal behaviour and energy usage patterns of the EWH.

The ambient temperature is controlled using a custom climatic regulation chamber equipped with two 500 W air heaters, circulation fans and venting fans. These actuators work together to regulate a user-defined chamber temperature. The platform has the ability to thermally emulate ambient temperatures up to 50 °C.

The temperature of the inlet water is regulated using a servo-controlled, three-port mixer valve. One of the inlet ports to the mixer is connected to a separate 100 L EWH device that is placed inside a standard chest freezer. The insulation of this tank is completely removed to decrease the thermal resistance between the chest freezer cavity and the water inside the tank. Therefore, if cold water is required for the experiment, the element of the tank will remain off and the chest freezer will switch on and cool the water inside the tank. Conversely, if warm water is required, the heating element of the tank switches on and heats up the water while the chest freezer is off. The second inlet port of the mixer valve is connected to the municipal water supply. A PI (proportional/integral) control system is used to regulate the temperature at the outlet port of the mixer valve. The temperature set point used in this case is the desired inlet water temperature to the main 150 L EWH device under test.

3.2. User emulation

The water usage patterns of the household user(s) have a substantial influence on the thermal behaviour of the EWH. Many studies focus on the development of stochastic water usage prediction algorithms, such as Heidari et al. [28] and Ritchie et al. [29]. A way to improve the accuracy of these models, is to generate more water usage profiles and the corresponding EWH energy response from the platform developed in this study.

This is accomplished by regulating the volumes, frequencies, flow rates and times of water usage events with an actuator (an electric ball valve) and two sensors: a digital flow meter that produces a digital pulse after sensing a specific volume of water and an outlet temperature sensor. The resolution of the volumetric flow sensor used is ± 2.5 mL.

The position of the electric ball valve is at the outlet of the tank to ensure that the EWH tank is pressurised to the regulated water line pressure when it is closed. In this setup, the water pressure is regulated to 100 kPa using a standard pressure regulator valve.

3.3. Electrical utility and thermostat emulation

Most electric water heaters utilise a standard thermostat that controls the electrical input to the heating element based on a sensed temperature and a user-defined set temperature. If the sensed temperature within the tank is below the set temperature, the thermostat will deliver electrical energy to the heating element, causing the water to heat up. The heating element will remain on and only switch off when the sensed temperature of the water has reached the desired set temperature with a small hysteresis band.

Literature has shown that the thermostat set point has a significant influence on the EWH energy characteristics [24] and the thermal stratification [12]. The experimental platform therefore incorporates the use of an electronically-controlled thermostat. A

custom digital controller receives the sensed temperature from the thermostat and determines the state of the heating element based on the desired set temperature defined in software. This allows for dynamic set point changes during an experiment and can be utilised by different heating control strategies.

The emulation of the electrical utility is also important. In South Africa there are rolling blackouts, a severe DM strategy, that cause many EWH units to be without electricity for up to 4 hours. A possible objective could be to observe the effects of these blackouts on the energy and stratification characteristics of the EWH. This is done by introducing an emulated power availability schedule in the controller.

Therefore, the platform's controller does two software checks for changing the state of heating element. The power availability schedule is checked to see if power is available from the emulated electrical utility and the sensed thermostat temperature is compared to the desired set temperature. This means that the heating element of the EWH could be off even when the sensed temperature is below the set temperature. This happens when there is no power available based on emulated utility availability schedule.

In the event of a possible controller fault and for safety reasons, the thermostat has a hardware cut-off temperature of 90 °C. This ensures that the temperature within the sensing region of the thermostat never exceeds this temperature.

In addition to this, a safety protocol is established to prevent the mid-region of the tank to exceed a temperature limit of 5 °C above the EWHs current set point temperature in the case of a faulty thermistor reading. This is done by implementing the temperature reading of a few of the mid-region DS18B20 sensors in the EWHs element actuating logic.

3.4. Data acquisition and sensor selection

An important objective of the platform is to sample experimental data that can aid in thermal and energy characterisation of the horizontal EWH. For this, the following measurements need to be taken: thermal stratification inside the tank using multiple internal temperature sensors, outlet water temperature for exergy analysis, environmental temperatures: ambient and inlet water, energy usage and volumetric flow rate of water.

In most studies, a uni-directional thermal stratification measurement strategy is used for vertical EWH experiments. However, the positional arrangement of the temperature sensors in this system allows for the measurement of vertical temperature variation and horizontal-radial temperature variation. In addition, the temperature variation along the length of the tank is also measurable. The three-dimensional sensor arrangement can be seen in Figure 3. This arrangement allows for the measurement of stratification in multiple regions of the horizontal tank. Thus, the thermal variation inside the tank can be measured in a three-dimensional space.

The stratification measurement system is designed to be placed inside of the 150 L tank. The tank is initially sectioned near the one end, closest to the heating element. This is followed by a flange assembly installation that allows the tank to be bolted shut after the stratification measurement system is positioned and secured inside. The metal flange of the sectioned tank can be seen in Figure 2b.

The thermal stratification is measured using nine temperature sensors that are mounted on modified and waterproofed rectangular aluminium tubes. They are equally-spaced and vertically arranged through the centre of the tank. This number is chosen based on similar work done in literature: Farooq et al. [14] placed eight equally-spaced temperature sensors along the height of a vertical tank wall, Fernandez-Seara et al. [13,20] mounted 11 equally-spaced thermocouples into their vertical tank, the vertical tank used by Kepplinger et al. [30] used 11 non-uniformly spaced thermocouples and Castell et al. [12] used 6 equally-spaced sensors positioned through the centre of their vertical tank. The resolution of the stratification data was suitable in all above-mentioned

studies. The application of 9 sensors is therefore considered to be sufficient, especially since it is for a horizontally-oriented tank.

The DS18B20 temperature sensor is specifically chosen based on its convenient digital *1-Wire* communication protocol, sensing accuracy, measurement range and resolution. These sensors have a measuring range of -55°C to 125°C and have a rated measurement error of ± 0.5 °C. However, for the range in which we measure, from 10°C to 70°C, the mean error in the datasheet is only ± 0.2 °C. An added advantage of this sensor is that the *1-Wire* communication protocol can support multiple devices on the same data line. This is ideal since there are fewer wires going into the pressurised tank. The design of the stratification measurement system implements eight separate data lines for the sake of modularity and fault detection convenience.

The sensor chip is encapsulated within a silicon-filled, stainless steel tube. The tube has a diameter of 6 mm with a length of 50 mm. The material properties of the stainless steel tube prevents the development of rust to a large extent. This is essential since these sensors would be exposed to heated and pressurised water for long periods of time.

3.5. Structural design considerations and suitability

The thermal stratification measurement system is designed to withstand the thermal fluctuations and pressure of the internal environment of the tank. Normal tank operating pressures can range from 100 kPa to 600 kPa in South Africa. The water temperature can fluctuate dramatically with temperatures typically ranging from 20 °C to 70 °C in different regions of the tank. This makes it difficult to place electronic sensors in this type of environment.

The support frame material is selected to be aluminium since it is light-weight, corrosion-resistant in water and has suitable thermal properties, such as high thermal conductivity and low specific heat capacity than that of water. The thermal conductivity and specific heat capacity of water are typically 0.598 W/mK and 4200 J/kgK, respectively. In contrast, the same properties of aluminium are typically 239 W/mK and 900 J/kgK respectively. The thermal conductivity property is a parameter used to quantify how well a material conducts heat and affects the rate at which heat is transferred. This parameter, along with the exposed surface area, has a direct influence on the transient thermal response time of the material. This relationship is described by Fourier's law of heat conduction shown in Equation 1,

$$\dot{Q}_{cond} = -kA_s \frac{dT}{dt} \tag{1}$$

where $\dot{Q}_{cond}$ is the rate of heat transfer through the material, k is the thermal conductivity of the material, A_s is the exposed surface area subjected to the heat transfer and $\frac{dT}{dt}$ is the rate of temperature change, also denoted as $\dot{T}$.

The aim of the frame is to provide rigid support for the sensors without influencing the true thermal response of the water inside the tank. Energy transfer between the water and the support frame material is inevitable. However, the aluminium frame does not act as a thermal reservoir which would cause slow thermal transients. The ability for water to store thermal energy is far greater than that of aluminium and conversely means that the aluminium tubes gain and lose thermal energy much faster than that of water. The presence of the aluminium thus has no significant impact on the slower thermal response of the body of water.

3.6. Digital system control

A custom controller for the system is designed to incorporate the use of an "over-the-counter" microcontroller such as an Arduino Due. This device is responsible for the control of the experimental platform. The controller is responsible for the control of environmental emulation, user behaviour emulation, electrical utility emulation and EWH thermostat control. It is also responsible for the data acquisition of the platform.

(a) **(b)**

Figure 2. Finalised thermal stratification measurement assembly (a) and tank installation inside of tank before tank is closed (b).

The data sampling parameters are configured and sent to the controller prior to the experiment. These parameters include sampling frequency, duration of experiment, set ambient air temperature, set geyser thermostat temperature and the set water inlet temperature. In addition, there is also the option of providing two types of schedules for EWH heating element power availability and water usage patterns. After the controller receives the experiment parameters, it then starts to set up the EWH environment, such as the set ambient air temperature if required. Once the environment is ready, the experiment starts and the time-stamped data is recorded to an SD card and streamed to a computer via a serial port.

The physical and finalised version of the stratification measurement system is shown in Figure 2. Each temperature bus module is connected to a three-core silicone cable that runs to the outside of the tank. For this to be possible, the existing anode rod had to be removed for the wires to have an entry point. Figure 2a shows how the cables are positioned in the tank. It was important to minimise the disturbance of typical flow into the tank, therefore the cables and the sensor busses were positioned appropriately to provide enough space from the inlet water diffuser.

3.7. Sensor referencing and geometry considerations

A referencing convention is established to make sense of the recorded data from the test station. There are 67 temperature sensors in total that are positioned at specific locations inside of the tank. Figure 3 shows the naming convention and sensor referencing notation for the sensors used for temperature variation measurement within the tank.

Most documented experimental stratification data from literature is captured and analysed for vertically-oriented tanks [11–14,20–22,31]. In these cases, the cross-sectional area as a function of height of the tank remains constant. This means that, assuming that the installed sensors are equally-spaced, the volume of the water measured for each sensor node will be the same. This is not the case for a horizontally-oriented tank since the cross-sectional area as a function of vertical height varies in a sinusoidal manner. The volume of water measured by the central node on the vertical plane (sensor position 4 on all sensor busses) is the largest as compared to the top and bottom layer volumes, which are equal and are the smallest.

This influences the way that the average temperature of the tank along the vertical plane is calculated. Since the nodal volumes for each vertically-positioned sensor are different, a weighted average calculation is more appropriate when the average temper-

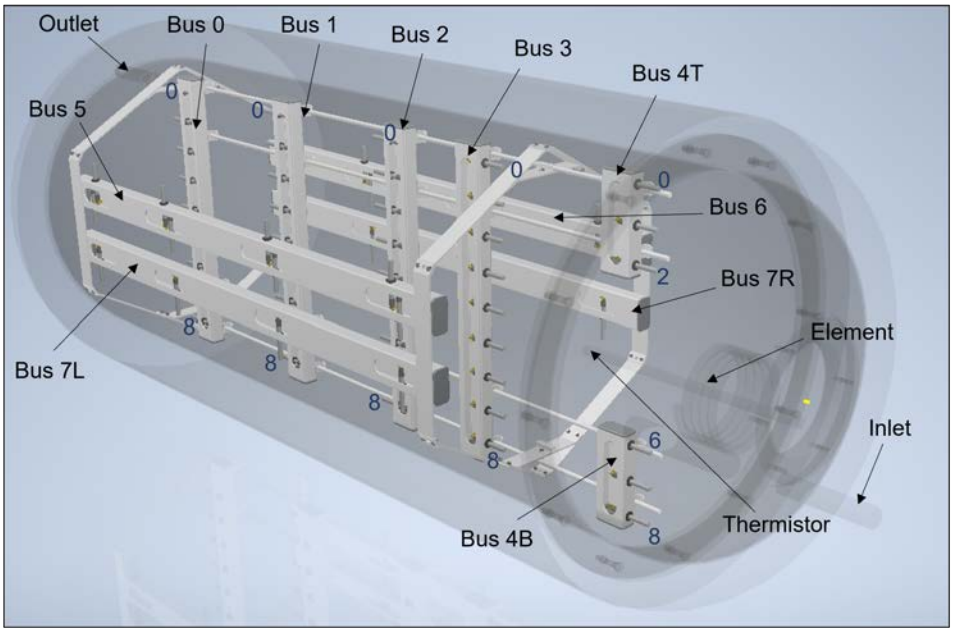

Figure 3. Reference diagram for sensor busses and locations. There are five vertically-oriented sensor "regions" along the longitudinal axis of the tank, (from Bus 0 at the outlet to Bus 4 at the inlet). Each region has nine sensors forming "layers" from top to bottom, labelled sensors 0 to 8. There are also four horizontally-oriented sensor buses measuring transversal distribution on the "sides", namely Bus 5 and 7L (left) and Bus 6 and Bus 7R (right). The reference notation for a specific sensor is be written as Bx,y where x is the bus number and y is the sensor position on bus x.

ature is required for analyses. Each nodal temperature that is measured in the vertical plane of the tank is multiplied by the volume of the measured region and divided by the total volume to act as a contribution factor. These 9 weighted values are added together to obtain the overall weighted average of the temperature in the tank at a specific point in time. The weighted average expression used is shown below in Equation 2.

$$T_{mean,vertical} = \frac{1}{V_{total}} \sum_{j=0}^{8} V_j \, T_j \tag{2}$$

where V_j and T_j are the nodal volume and measured temperature at sensor j, respectively.

For the physical design shown in Figure 3, the nodal volumes for each sensed region in the vertical plane is tabulated below in Table 1. It is important to note that when these volumes are used to calculate the weighted average of the vertical temperature variation the tank, the assumption is made that the longitudinal and transverse temperature variation along the length, and along the horizontal radius of the tank is negligible and can be ignored. The volumetric-weighted temperature average is determined and visualised in Section 4 for each longitudinal position in the tank.

4. Results

The test station is evaluated through its ability to (1) sample data of three-dimensional thermal variation in the EWH tank for static and dynamic modes of operation and the associated energy consumption, (2) emulate a user-defined environment which includes a set temperature for emulated ambient temperature and inlet water temperature, and (3) follow a predefined water usage and electrical availability schedule.

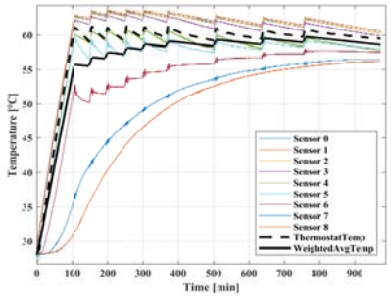

(a) Region 0 (Outlet)

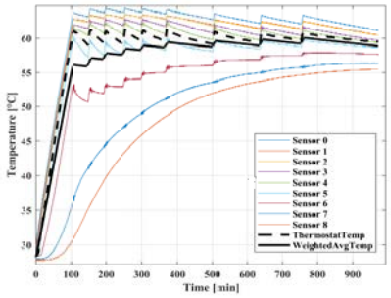

(b) Region 1

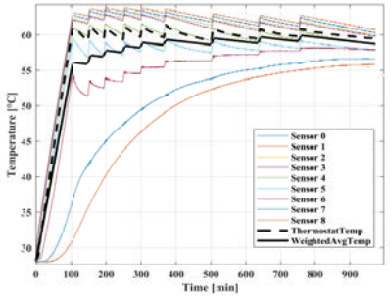

(c) Region 2 (Middle)

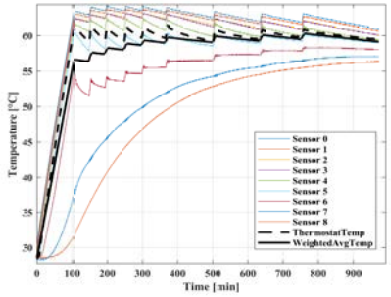

(d) Region 3

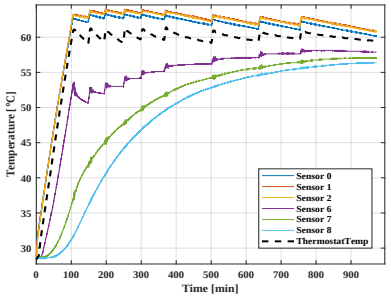

(e) Region 4 (Inlet)

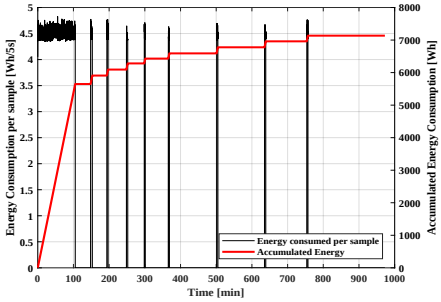

(f) Energy measurements

Figure 4. Static temperature variation in the EWH along the height of the tank, predominantly due to stratification, at different longitudinal regions from the outlet (a) to the inlet (e), with no water draw.

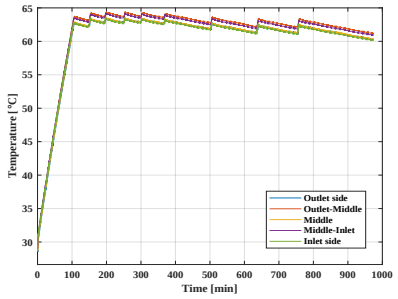

(a) Layer 0 (Top)

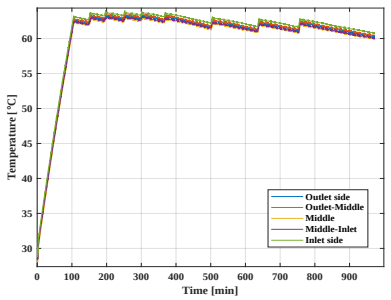

(b) Layer 2

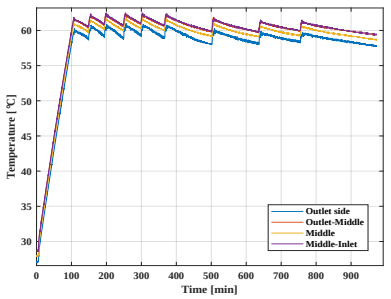

(c) Middle layer – sensor location 4

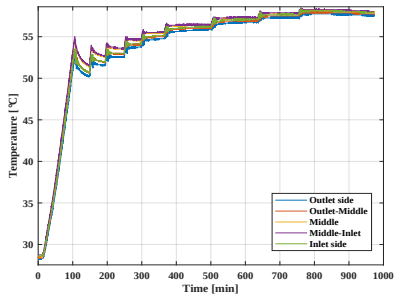

(d) Layer 6

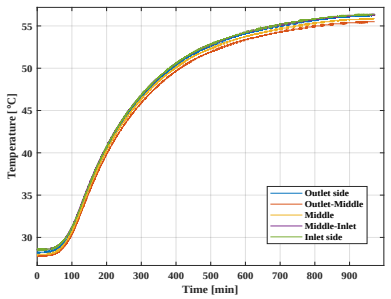

(e) Layer 8 (Bottom)

Figure 5. Static temperature variation in the EWH along the longitudinal axis of the tank at different layers ranging from the top (layer 0) to the bottom (layer 8), with no water draw. *Note that the inlet side of the tank (region 4) does not have a middle temperature sensor as that location is occupied by the heating element.*

Layer	Volume
V_0	$9.42L$
V_1	$15.69L$
V_2	$18.84L$
V_3	$20.51L$
V_4	$21.08L$
V_5	$20.51L$
V_6	$18.84L$
V_7	$15.69L$
V_8	$9.42L$

Table 1: Volumes (based on design geometry) for each layer from sensor 0 at the top to sensor 8 at the bottom.

4.1. Static heating and cooling (No water draw)

The EWH was subjected to a thermostatically-controlled heating process, with a 60 °C set point and an initial bulk temperature of 28 °C. The measured thermostat temperature and weighted temperature average are shown in Figure 4. During the initial heating process, most of the upper layers in the tank exhibited a constant heating rate of approximately 0.31 °C/min, while the bottom three layers had a slower thermal response during the heating process. This is true for every longitudinal position measured along the length of the tank. Figure 4 shows that layers 7 and 8 have much slower thermal responses than the immediate upper layers. The temperature measured at layer 6 reaches a relatively constant heating rate (similar to the upper regions of the tank), but has an initial delayed response of about 15 min.

The temperatures measured at the inlet region, where the element and thermostat also are, show that the temperature sensed by the thermostat, which is used as the feedback temperature for the element switching, is substantially different at the different heights. At the time step when the sensed thermostat temperature reaches the EWH set point of 60 °C, the top layer is measured to be 62.25 °C, while the bottom layer is measured to be 30.8 °C. This means that at the point where the set point of the tank is reached, there is still a temperature difference of at least 30 °C between the top and bottom layer. The weighted average temperature at the time when the thermostat switches off, is 56.5 °C at the middle-inlet longitudinal region of the tank.

As the sensed thermostat temperature is regulated, the lower layers of the tanks slowly heat up towards the set point temperature. Since the temperature gradient between the upper and lower regions of the tank is initially high, it induces a high heat transfer rate between these layers, as per Equation 1. This is due to the decay of the temperature gradient between the upper and the lower regions of the tank. Consequently, thermal energy is lost from the top layers (and equivalently gained by the bottom layers) faster at the start of the temperature regulation phase. This is evident when analysing the switching frequency of the thermostat in Figure 4, which was more than double between 100 and 250 min that observed from 500 and 750 min.

The longitudinal temperature variation along the length of the tank, for same heating experiment, is shown in Figure 5. It is visually clear that there is no significant temperature variation along the length of the tank. Figures 5 (a) to (c) clearly show the regulated dead band and its switching frequency. Figure 5 (d) shows some indication of switching, indicated by the sharp temperature changes, and also a slow temperature rise response. This could indicate that, immediately after the sensed temperature reached the dead band region, the rate of heat transfer from this layer to the layers below was higher than that of the heat gained from the layers above. As the layers below heated up, the heat transfer rate from the upper layers to this layer became larger, causing a smoother and slow rise in temperature. Figure 5 (e) again shows the slow thermal response of the

bottom layer of the tank. Note that sensor location 6, shown in Figure 5(e), exhibits a combination of thermal behaviours observed in both Figure 5 (c) and (e).

An interesting thermal response was noticed while measuring the horizontal-transverse temperature variation at the bottom layers of the tank. Figure 6 shows the horizontal-transverse temperature variation of the top, middle and bottom regions of the tank at different longitudinal positions. From this data, it is clear that the transverse temperature variation at the upper and middle regions of the tank is practically insignificant during a heating and thermostatically-controlled experiment.

However, at the lower region of the tank, a significant temperature variation is observed near the inlet side of the tank. At the time that when the thermostat sensor reaches the set point of 60 °C, the temperature near the inlet port of the tank (on the right side as per Figure 3) is measured to be approximately 45 °C while the middle and left sensors at the same vertical and longitudinal position measures a temperature of 54 °C. This thermal behaviour is less pronounced at the outlet side of the tank. One possible reason for this observed thermal behaviour could be the influence of the colder water at the right-of-centre inlet port of the tank. There is a clear temperature gradient between this region and the water at the inlet which induces a thermal exchange, causing a slower temperature response.

4.2. Dynamic mode (Water draw)

A dynamic test was conducted to visualise the vertical movement of the thermocline and the degree of stratification when water is discharged from a charged (heated) tank. The test was conducted using a water discharge rate of 8 L/min and a starting temperature of approximately 53 °C. The results of the vertical temperature variation are shown in Figure 7, which shows the temperature variation of all nine measured layers and the weighted temperature average between them for different longitudinal position. The valve was opened 50 seconds after the data capturing started. The tank was fully discharged after about 20 min, and the valve was closed again after 28 min of water discharge.

The timing of the falling slopes in Figure 7 show that the rate at which the thermocline moves from the bottom to the top at a relatively similar rate between layers 1 and 6 for all longitudinal positions in the tank. The gradients of the slopes in the figure show that the rate of temperature decay is also similar for layers 1 to 8. However, there is a significant difference in response time at the upper region (sensor location 0) of the tank than the lower regions. Separately, the rate of temperature decay in the top layer (sensor location 0) at the inlet side of the tank is markedly different than the temperature decay of the same layer at the outlet side. The decay rate of of the top layer at the outlet side of the tank is the same as its neighbouring layers – Figure 7 a–d. However, at the inlet side of the tank, the decay rate is slower since it stays warmer for a longer period of time – Figure 7e. This observation is better visualised in Figure 8a . From this visualisation, it is clear that the temperature in the top layer is the highest at the inlet side and becomes sequentially cooler moving towards the outlet side of the tank.

A possible reason for this observation is the presence of a local rotating vortex that exists at the top corner of the inlet side of the tank caused by the flow dynamics and geometry of the tank. A similar observation was made by Abdelhak, et al. [21], who concluded, based on their CFD analyses, that the presence of this vortex decreases the overall efficiency of the tank because it draws thermal energy away from the outlet region of the tank – decreasing the discharge efficiency.

Figure 8a shows that the top layer exhibits another interesting characteristic right after the valve is closed. The top layer temperature at the outlet region of the tank suddenly increased in temperature by at least 1 °C. From this, the presence of a vortex is further supported based on the hypothesis that the sudden stop in dynamic flow (valve closing) would allow the fluid from the warmer vortex region to move and/or diffuse to the outlet side.

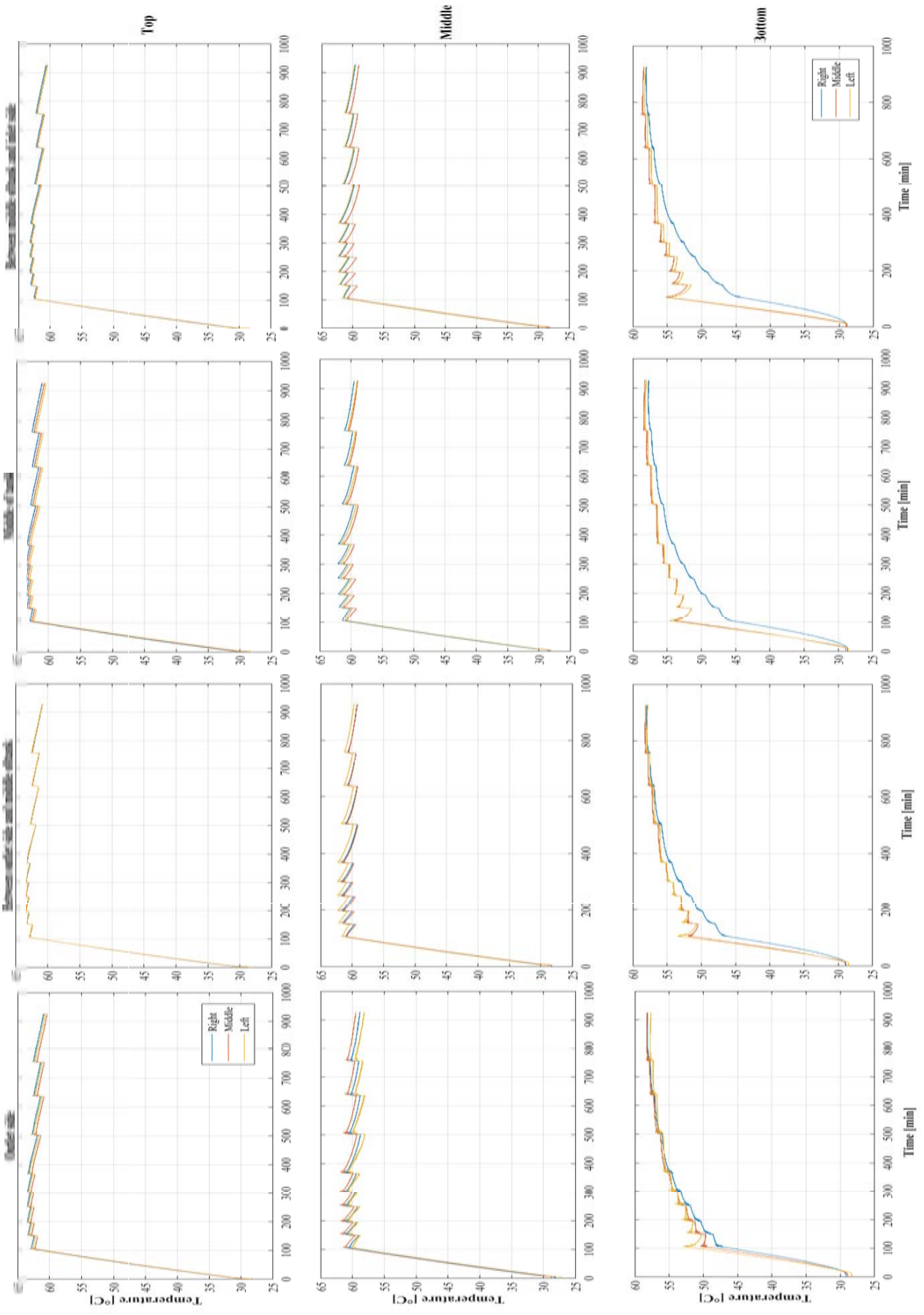

(f)

Figure 6. Transverse temperature variation for 60 °C thermostatically-controlled (TC) experiment at different longitudinal positions along the tank (a) the outlet side (bus region 0), (b) Outlet-Middle (Bus region 1), (c) Middle of tank (bus region 2) and (d) Middle-Inlet (bus region 3) - close to the inlet side of the tank.

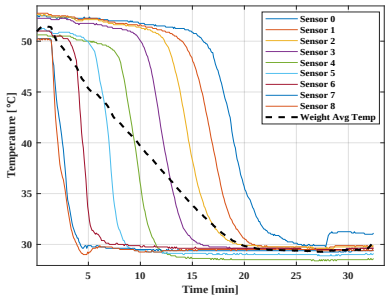

(a) Region 0 (Outlet)

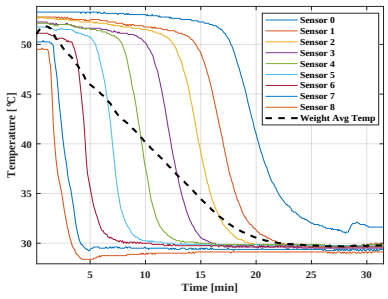

(b) Region 1

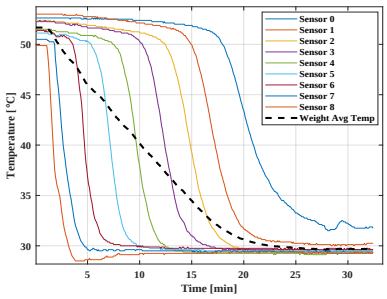

(c) Region 2

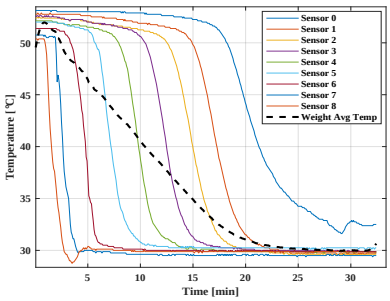

(d) Region 3

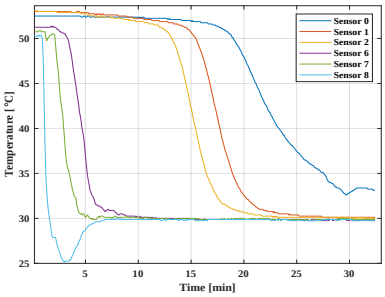

(e) Region 4 (Inlet)

Figure 7. Dynamic temperature variation in the EWH along the height of the tank at different longitudinal regions from the outlet (a) to the inlet (e), with water draw.

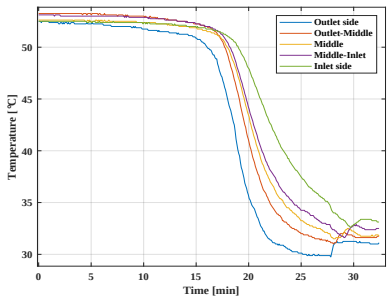

(a) Layer 0 (Top)

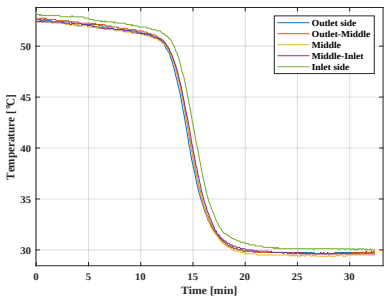

(b) Layer 2

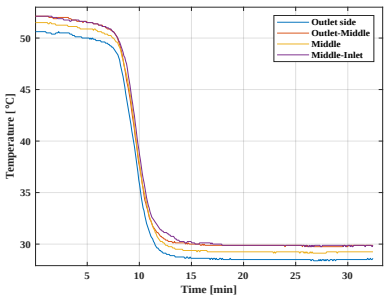

(c) Layer 4

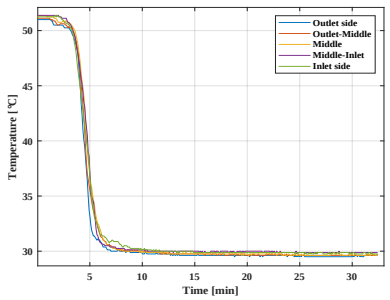

(d) Layer 6

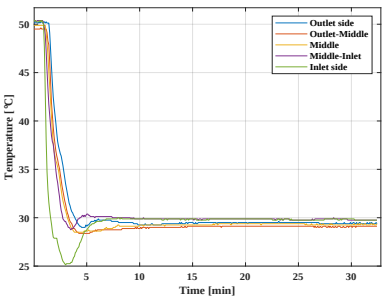

(e) Layer 8 (Bottom layer)

Figure 8. Dynamic temperature variation in the EWH along the longitudinal axis of the tank at different layers ranging from the top (layer 0) to the bottom (layer 8), with no water draw. *Note that the inlet side of the tank (region 4) does not have a middle temperature sensor as that location is occupied by the heating element.*

Figure 8e shows the longitudinal temperature variation for the same experiment at the bottom layer of the tank. There is a significant drop in temperature recorded at the inlet side of the lower layer. This temperature response represents the variation in temperature experienced near the inlet port. The variation is caused by different pipe locations inside and outside the laboratory. The initial average temperature of the water in the pipe network (inside the laboratory) was 25 °C followed by a later average water temperature of 30 °C, which in this case was the settling point of the temperature in the tank. Inlet temperature control was disabled for this experiment.

4.3. Energy measurement

The energy required to heat up the water within the tank is a function of volume, specific heat, density and the temperature change. The density and the specific heat properties of water are both functions of temperature. Thus, in order to have a more accurate calculation of the energy required, the integral of the density and specific heat functions over the temperature range is calculated and multiplied by the tank volume. The equation is shown in Equation 3.

$$\int_{T_1}^{T_2} dE = V \int_{T_1}^{T_2} \rho_w(T) c_{p,w}(T) dT \tag{3}$$

where $\rho_w(T)$ and $c_{p,w}(T)$ are expressed in $\frac{\text{kg}}{\text{m}^3}$ and $\frac{\text{J}}{\text{kgK}}$, respectively and are shown in Equations 4 and 5. Temperature units in these expressions are in Kelvin.

$$\rho_w(T) = \frac{1}{0.00149343 - 3.7164 \times 10^{-6} T + 7.09782 \times 10^{-9} T^2 - 1.90321 \times 10^{-20} T^6} \tag{4}$$

$$c_{p,w}(T) = 8155.9 - 20.80627T + 0.0511283T^2 - 2.17582 \times 10^{-13} T^6 \tag{5}$$

To validate the energy measurement of the platform, a simple experiment was carried out in which we measured the amount of energy needed to heat up the tank water from a uniform temperature of 28 °C to a set temperature of 60 °C. Theoretically, the total energy required for a single 150 L EWH to heat up from 28°C to 60°C is calculated using Equations 3, 4 and 5 and is given by

$$E = 0.15 \int_{28+273.15}^{60+273.15} \rho(T) c_p(T) dT \left(\frac{1\ \text{W h}}{3600\ \text{J}} \right) = 5518.2\ \text{W h} \tag{6}$$

The corresponding energy measurements of the experiment are shown in Figure 4f. The time required to heat up the tank from its initial temperature to its set point was approximately 102 min. At the time when the thermostat temperature reached 60 °C, the recorded accumulated energy was 5505 W h.

When comparing the theoretical energy input requirement from Equation 3 to the measured results shown in Figure 4f, the accuracy is calculated to be 99.76 %. Based on this, the energy measurements are validated and can be used for further analyses.

5. Conclusion

Demand management strategies that rely on the direct control of electric water heaters, with their inherent potential for storing thermal energy, aim to reduce electrical load, reduce thermal losses, and to ensure user satisfaction (hot water) without fostering bacterial growth that occurs at lower temperatures. Their efficacy therefore relies on an accurate representation of the internal temperature distributions of these heaters. Although the internal temperature distribution of electric water heaters have been characterised for the vertical orientation, they have not been characterised for the horizontal orientation, which is more common in developing countries.

We presented a fully controllable platform with which the thermal behaviour of a horizontal water heater can be characterised under a wide range of environmental

conditions (e.g. ambient temperature and inlet water temperature), control parameters (e.g. heating schedule, thermostat set temperature), and user behaviour (flow rate and draw volume). We presented the internal temperature measurements under static conditions (no water drawn) when the heater was heating from cold and kept at a set temperature. These were repeated under dynamic conditions (water drawn).

The static results show the dominant impact of stratification on the temperatures inside the tank, with the higher layers heating substantially faster than the lower ones. The thermal response of the three bottom layers were considerably slower than the layers immediately above. This is in contrast with what has been documented in literature for vertically-oriented tanks [12,14,32]. It is believed that the location of the heating element and tank geometry have an influence on this recorded difference.

This thermal stratification also had an impact on the element switching frequency, of which is higher shortly after the first heating cycle, and then slower as the bottom layers heat up. The longitudinal differences in stratification were observed to be minor, with only the the middle layer varying by more than 2 °C from the inlet to the outlet. The differences between the two sides (left and right) of the water heater were mostly symmetrical for the middle and top layers. However, the inlet pipe, which is placed at a slight offset to the right, had a marked cooling thermal exchange impact on the right side of the bottom layer in static conditions, which extends even to the middle region along the longitudinal axis.

The dynamic results showed the introduction of the thermocline and its subsequent movement upwards in the tank to the top layer. Interestingly, the inlet region's upper layer took the longest to cool down. An interesting phenomenon was observed in which the temperature at the outlet rose for a few minutes after valve was closed. We believe this may be a thermal exchange from the trapped heat in the fluid-driven vortex at the top layer, near the inlet side of the tank.

Acknowledgements

We thank the following organisations for funding: MTN (S003061) and Eskom (TESP:2020).

References

1. Van Schalkwyk, P.D.; Engelbrecht, J.A.A.; Booysen, M.J. Inside and out: A Platform to Characterise Stratification in Horizontal Electric Water Heaters. 2021 International Conference on Electrical, Computer and Energy Technologies (ICECET), 2021, pp. 1–7. doi: 10.1109/ICECET52533.2021.9698517.
2. Yildiz, B.; Bilbao, J.I.; Roberts, M.; Heslop, S.; Dore, J.; Bruce, A.; MacGill, I.; Egan, R.J.; Sproul, A.B. Analysis of electricity consumption and thermal storage of domestic electric water heating systems to utilize excess PV generation. *Energy* **2021**, *235*, 121325. doi: 10.1016/j.energy.2021.121325.
3. Tejero-Gómez, J.A.; Bayod-Rújula, A.A. Energy management system design oriented for energy cost optimization in electric water heaters. *Energy and Buildings* **2021**, *243*, 111012.
4. Roux, M.; Apperley, M.; Booysen, M.J. Comfort, peak load and energy: Centralised control of water heaters for demand-driven prioritisation. *Energy for Sustainable Development* **2018**, *44*, 78–86. doi:10.1016/j.esd.2018.03.006.
5. Hohne, P.A.; Kusakana, K.; Numbi, B.P. A review of water heating technologies: An application to the South African context. *Energy Reports* **2019**, *5*, 1–19. doi:10.1016/j.egyr.2018.10.013.
6. International Energy Agency. *World Energy Outlook 2018*; 2018; p. 661. doi:10.1787/weo-2018-en.
7. Diao, R.; Lu, S.; Elizondo, M.; Mayhorn, E.; Zhang, Y.; Samaan, N. Electric water heater modeling and control strategies for demand response. 2012 IEEE Power and Energy Society General Meeting, 2012, pp. 1–8. doi:10.1109/PESGM.2012.6345632.
8. Roux, M.; Apperley, M.; Booysen, M.J. Comfort, peak load and energy: Centralised control of water heaters for demand-driven prioritisation. *Energy for Sustainable Development* **2018**, *44*, 78–86. doi:10.1016/j.esd.2018.03.006.
9. Xu, Z.; Diao, R.; Lu, S.; Lian, J.; Zhang, Y. Modeling of Electric Water Heaters for Demand Response: A Baseline PDE Model. *IEEE Transactions on Smart Grid* **2014**, *5*, 2203–2210. doi: 10.1109/TSG.2014.2317149.

10. Stone, W.; Louw, T.; Gakingo, G.; Nieuwoudt, M.; Booysen, M.J. A potential source of undiagnosed Legionellosis: Legionella growth in domestic water heating systems in South Africa. *Energy for Sustainable Development* **2019**, *48*. doi:10.1016/j.esd.2018.12.001.
11. Chandra, Y.P.; Matuska, T. Stratification analysis of domestic hot water storage tanks: A comprehensive review. *Energy and Buildings* **2019**, *187*, 110–131. doi:10.1016/j.enbuild.2019.01.052.
12. Castell, A.; Medrano, M.; Solé, C.; Cabeza, L.F. Dimensionless numbers used to characterize stratification in water tanks for discharging at low flow rates. *Renewable Energy* **2010**, *35*, 2192–2199. doi:10.1016/J.RENENE.2010.03.020.
13. Fernández-Seara, J.; Uhía, F.J.; Sieres, J. Experimental analysis of a domestic electric hot water storage tank. Part I: Static mode of operation. *Applied Thermal Engineering* **2007**, *27*, 129–136. doi:10.1016/j.applthermaleng.2006.05.006.
14. A. A. Farooq.; A. Afram.; N. Schulz.; F. Janabi-Sharifi. Grey-box modeling of a low pressure electric boiler for domestic hot water system. *Applied Thermal Engineering* **2015**, *84*, 257–267. doi:10.1016/j.applthermaleng.2015.03.050.
15. Dolan, P.S.; Nehrir, M.H.; Gerez, V. Development of a Monte Carlo based aggregate model for residential electric water heater loads. *Electric Power Systems Research* **1996**, *36*, 29–35. doi:10.1016/0378-7796(95)01011-4.
16. Kondoh, J.; Lu, N.; Hammerstrom, D.J. An Evaluation of the Water Heater Load Potential for Providing Regulation Service. *IEEE Transactions on Power Systems* **2011**, *26*, 1309–1316. doi:10.1109/TPWRS.2010.2090909.
17. Leeuwner, L.L.; Booysen, M.J.; Visagie, L. Evaluation of the Energy Model of a Horizontally-Mounted Electric Water Heater Through Internal Temperature Measurement **2017**.
18. Engelbrecht, J.A.A.; Ritchie, M.J.; Booysen, M.J. Optimal schedule and temperature control of stratified water heaters. *Energy for Sustainable Development* **2021**, *62*, 67–81. doi:10.1016/j.esd.2021.03.009.
19. Nel, P.J.C.; Booysen, M.J.; van der Merwe, B. A Computationally Inexpensive Energy Model for Horizontal Electric Water Heaters With Scheduling. *IEEE Transactions on Smart Grid* **2018**, *9*, 48–56. doi:10.1109/TSG.2016.2544882.
20. Fernández-Seara, J.; Uhı´a, F.J.; Sieres, J. Experimental analysis of a domestic electric hot water storage tank. Part II: dynamic mode of operation. *Applied Thermal Engineering* **2007**, *27*, 137–144. doi:10.1016/j.applthermaleng.2006.05.004.
21. Abdelhak, O.; Mhiri, H.; Bournot, P. CFD analysis of thermal stratification in domestic hot water storage tank during dynamic mode. *Building Simulation* **2015**, *8*, 421–429. doi:10.1007/s12273-015-0216-9.
22. Rosen, M.A. The exergy of stratified thermal energy storages. *Solar Energy* **2001**, *71*, 173–185. doi:10.1016/S0038-092X(01)00036-6.
23. Armstrong, P.; Ager, D.; Thompson, I.; McCulloch, M. Domestic hot water storage: Balancing thermal and sanitary performance. *Energy Policy* **2014**, *68*, 334–339. doi:10.1016/j.enpol.2014.01.012.
24. Booysen, M.J.; Cloete, A.H. Sustainability through Intelligent Scheduling of Electric Water Heaters in a Smart Grid. 2016, pp. 848–855. doi:10.1109/DASC-PICom-DataCom-CyberSciTec.2016.145.
25. Ritchie, M.J.; Engelbrecht, J.A.A.; Booysen, M.J. Centrally Adapted Optimal Control of Multiple Electric Water Heaters. *Energies* **2022**, *15*. doi:10.3390/en15041521.
26. Kizilors, C.; Aydin, D. Effect of thermostat position and its set-point temperature on the performance of a domestic electric water heater. *International Journal of Low-Carbon Technologies* **2021**, *15*, 373–381. doi:10.1093/IJLCT/CTAA007.
27. Nel, P.J.C.; Booysen, M.J.; van der Merwe, B. Saving on household electric water heating: What works best and by how much? 2017 IEEE Innovative Smart Grid Technologies - Asia (ISGT-Asia), 2017, pp. 1–6. doi:10.1109/ISGT-Asia.2017.8378439.
28. Heidari, A.; Olsen, N.; Mermod, P.; Alahi, A.; Khovalyg, D. Adaptive hot water production based on Supervised Learning. *Sustainable Cities and Society* **2021**, *66*, 102625. doi:10.1016/j.scs.2020.102625.
29. Ritchie, M.J.; Engelbrecht, J.A.A.; Booysen, M.J. A probabilistic hot water usage model and simulator for use in residential energy management. *Energy and Buildings* **2021**, *235*. doi:10.1016/j.enbuild.2021.110727.

30. Kepplinger, P.; Huber, G.; Preißinger, M.; Petrasch, J. State estimation of resistive domestic hot water heaters in arbitrary operation modes for demand side management. *Thermal Science and Engineering Progress* **2019**, *9*, 94–109. doi:10.1016/j.tsep.2018.11.003.
31. Kepplinger, P.; Huber, G.; Preißinger, M.; Petrasch, J. State estimation of resistive domestic hot water heaters in arbitrary operation modes for demand side management. *Thermal Science and Engineering Progress* **2019**, *9*, 94–109. doi:10.1016/j.tsep.2018.11.003.
32. Fernández-Seara, J.; Uhía, F.J.; Sieres, J. Experimental analysis of a domestic electric hot water storage tank. Part I: Static mode of operation. *Applied Thermal Engineering* **2007**, *27*, 129–136. doi:10.1016/j.applthermaleng.2006.05.006.